Research Open

Geology, Earth and Marine Sciences

Volume 7 Issue 6

Research Article

Diamond in Pegmatites and Related Rocks in the Upper Crust

Rainer Thomas*

Im Waldwinkel 8, D-14662 Friesack, Germany

***Corresponding author:** Rainer Thomas, Im Waldwinkel 8, D-14662 Friesack, Germany

Received: September 30, 2025; **Accepted:** October 02, 2025; **Published:** October 05, 2025

Abstract

We show that the general absence of the graphite G-band typically characterizes classic diamonds formed in Earth's mantle. Diamonds, which are transported via supercritical fluids or melts from the mantle region into the crust, generally show the typical graphite G-band. The intensity of this band is clearly dependent on the laser energy used on the sample. That also applies to diamonds formed directly in crustal regions (e.g., in pegmatites) or for diamonds grown in grey cast iron.

Keywords: *Diamonds, Raman spectroscopy, Differences in the Raman spectra, Origin of the G-band*

Introduction

In a row of papers, the author, with his coauthors [1,2], has shown that diamonds or DLCs (diamond-like carbon) can be brought with supercritical fluids or melts (SCF or SCM) from mantle depths to the Earth's crust, primarily as spherical crystals. Later, we have seen [3] that DLC can form directly at crustal regions, often as small crystals or whiskers in many different minerals (beryl, quartz, topaz, cassiterite, fluorite, zinnwaldite, and others). By the finding of diamonds in grey cast iron [4,5], formed at an apparent low pressure, we saw significant differences in the Raman spectrometric behavior of such diamonds, or better, DLCs. The main difference in behavior is seen in the FWHM (Full-Width at Half Maximum) and in the position of the first-order diamond line, which is about 1332.5 cm^{-1} for the undoped and undisturbed diamond lattice [6]. According to the same author, MWCVD diamond powder has a double peak at 1325 and 1330 cm^{-1} for a mixture of hexagonal and cubic phases, respectively. MWCVD refers to fine diamond particles, or diamond powder, that is created or used in conjunction with a Microwave Plasma Chemical Vapor Deposition (MWCVD) process. Large values for FWHM are typical for an increase in the defect density and for nanodiamonds [7]. However, most diamonds found in mineralization in the crust region are greater than 2 µm in diameter; therefore, alone, the origin of the FWHM increase by small nanodiamonds is not the origin. According to Prawer et al. (1998) [7], the Raman cross-section for sp^2 clusters (C=C) carbon is significantly greater (by a factor of 50) than for sp^3-bonded structures. That means graphite, as a simplification, is easy to excite.

Samples and Methods

Natural Samples and Diamonds are Used for Cutting, Grinding, and Polishing

To demonstrate that diamonds, which are used for cutting, grinding, polishing, and jewelry, do not show such energy-dependent behavior, some such diamonds are also used (see Thomas et al., 2023). Generally, we used for the study of natural samples (beryl, quartz, topaz, cassiterite, fluorite) free double-polished thick sections (300 – 500 µm thick). In the case of the mica zinnwaldite, we used simple cleavages of mica. The samples come from granites, pegmatites, and vein mineralizations from the Variscan Erzgebirge. Another sample is a quartz ship from the Froland pegmatites in Norway. With these diamonds (DLCs), we can show the influence of the laser power on the sample, which classic diamonds do not show.

Microscopy, Raman Spectroscopy

Besides a polarization microscope for transmission and reflection (JenaLab Pol), which is equipped with a universal stage and different microscope rotary compensators, sophisticated mineralogical studies are possible. We performed all routine microscopic and Raman spectroscopic studies with a petrographic polarization microscope (BX 43) with a rotating or XY stages coupled with the EnSpectr Raman spectrometer R532 (Enhanced Spectrometry, Inc., Mountain View, CA, USA) in reflection and transmission. The Raman spectra were recorded in the spectral range of 0–4000 cm^{-1} using an up to 50 mW single-mode 532 nm laser, an entrance aperture of 20 µm, a holographic grating of 1800 g/mm, and a spectral resolution of 4 cm^{-1}. Detailed descriptions of the methods used are given by Thomas et al. (2025a and 2025b) [4,5]. From our studies [5], we found that the measuring spot at the sample using the high-quality 100x objective is ~ 1µm. From this, a high energy density results (converted: 4000 W/cm^2) at 30 mW. To prevent intense heating during the measurement and formation of sp^2 carbon, we used 0.5 to 4 mW on the sample and, for fast routine measurements, 30 mW.

Experimental Section

To demonstrate the laser energy-dependent behaviours of some diamonds, we take the Raman spectra of the first-order diamond line at 30 and 4 mW, if a graphite band is visible. A row of natural and synthetic diamonds does not show any signs of a graphite band around 1580 cm^{-1} (Table 1).

More information is in Table 1 in Thomas et al. (2023a). All listed diamonds show no graphite band.

Results and Discussion

Generally, all diamonds found in the upper Earth crust formed there or brought with supercritical fluids or supercritical melts show, when using laser energy of 30 mW (see Table 1), a strong Raman band of graphite near 1580 cm^{-1}. We have also seen in the case of the formation of diamonds, in grey cast iron (Thomas et al. 2025), at low bulk pressure, and, possibly, high temperatures, that they have a huge FWHM and exhibit metastable behaviour under the laser light (e.g., Figure 2 in Thomas et al. (2025b) [9]. It is very instructive to see this in the two Raman spectra from the Froland pegmatite quartz (Figure 1a and 1b) – here as a natural sample.

From both figures, we see the influence of laser energy on the sample. The diamond is black and obviously contains carbon. Therefore, the graphite band does not vanish completely. In Table 2 are some results arranged that show a developed, mostly strong graphite G-band beside the diamond band.

Thomas has shown [9] that graphite is widespread in many minerals formed during the Variscan time in the Erzgebirge. In the past, that has been ignored up to now. Furthermore, Thomas et al. (2023a) [1] have shown that supercritical fluids (SCFs) and melts (SCMs) are very active in the Variscan time in the Erzgebirge and other places and have brought water, methane, hydrogen, and also different ore elements (e.g., B, Be, Cs, Sn) into the Earth's crust. That is also valid for other times, such as the Precambrian (Bornholm, Norway, Ukraine). Opposite to gray cast iron, methane and hydrogen are not rare components in nature at high temperatures [13] and in supercritical fluids. So, the supercritical phases are rich in methane [2], which is also supercritical [14,15]. Such fluids can penetrate all minerals, their channels, or grain boundaries. If they meet, for example, carbon/graphite, they can then form moissanite (in beryl) and/or diamonds [2]. As an example, we show here a case of a diamond-like compound found in fluorite in zinnwaldite from Zinnwald. Figures 2a and 2b show the spectrum of those spherical lonsdaleite crystals [3] taken at different laser energies.

Table 1: Natural and synthetic diamonds without a graphite band (small selection), 30 mW on sample.

Origin	First-order diamond line (cm^{-1})	FWHM (cm^{-1})	n
Natural diamonds			
Brazil 2453/37	1332.2 ± 0.4	4.3 ± 0.4	20
Koffiefontein mine/South Africa	1328.0 ± 2.7	23.1 ± 9.3	15
Sierra Leone, Sewa River	1332.0 ± 0.4	5.4 ± 0.1	10
Udatshnaya, Sibiria	1329.7	10.4	1
Red Diamond, Sibiria	1332.6 ± 0.2	4.8	10
Red Diamond, Sibiria, black incl.	1332.2 ± 0.5	5.2 ± 0.4	10
W-Australia, Argyle Mine	1332.3 ± 0.5	5.8 ± 0.9	10
Synthetic diamonds			
HDAC-diamond (Bassett, 2009) [8]	1331.6 ± 0.6	5.2 ± 0.2	10
ZIPE Potsdam (black), GDR	1333.1 ± 0.9	8.9 ± 1.9	10
Diamond cutting disks			
Belgium	1332.8 ± 0.3	4.9 ± 0.1	10
Russia	1331.8 ± 0.3	4.6	10
Diamond Paste for metallography (Struers B)			
	1331.5 ± 0.6	5.5 ± 0.2	8

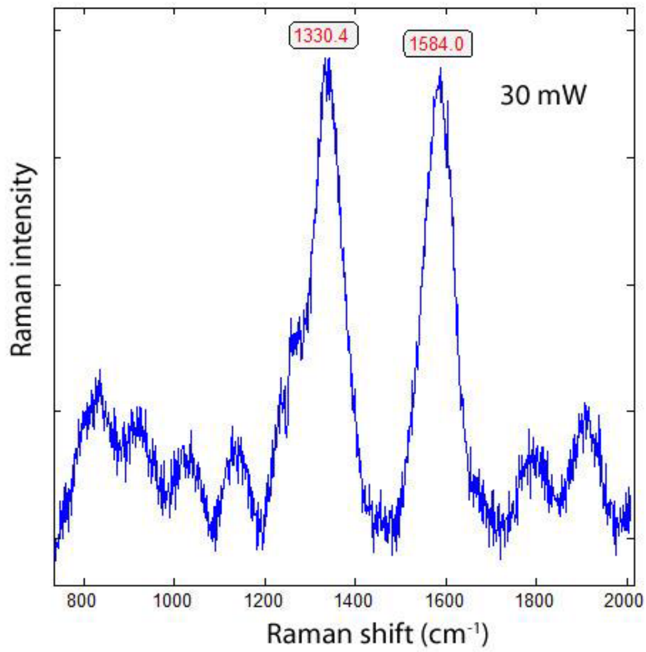

Figure 1a: Raman spectrum of DLC in pegmatite quartz from Froland/S-Norway taken at 30 mW.

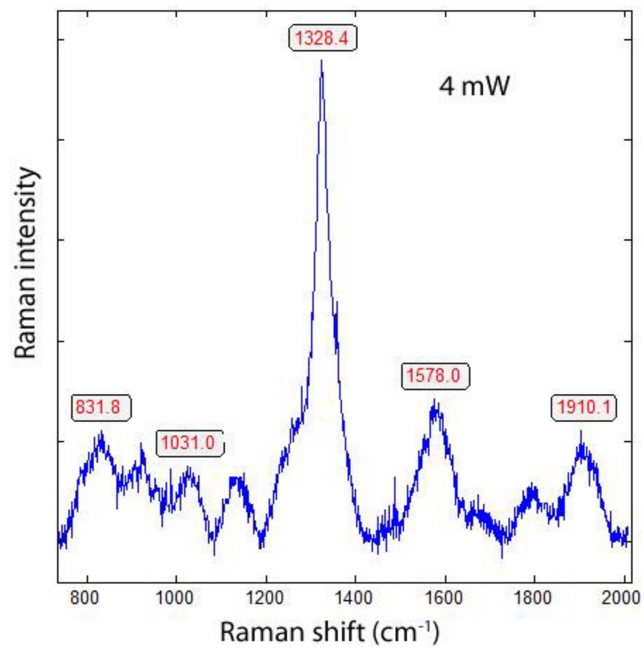

Figure 1b: Raman spectrum of the same DLC in pegmatite quartz from Froland/S-Norway, here, however, taken at 4 mW.

Table 2: Diamonds transported via SCF/SCM into the upper Earth crust or formed there (a selection). [~30 mW]. For comparison, the results for the grey cast iron sample No. 2 are given.

Origin	D-line (cm^{-1})	FWHM (cm^{-1})	n	G-line (cm^{-1})	FWHM (cm^{-1})	n	References
Bornholm, Pegmatitic quartz	1315.6 ± 0.2	65.0 ± 1.2	30	1564.8 ± 7.3	76.0 ± 6.02	10	Thomas (2024) [10]
Zinnwald Granite ZW 212	1328.5 ± 4.3	63.1 ± 18.0	19	1578.7 ± 7.2	57.5 ± 13.5	19	Thomas (2025)
Zinnwald, Pegmatitic quartz	1321.6 ± 7.0 1321.6 ± 3.8	14.3 ± 0.8 51.6 ± 6.7	14 12	1575.6 ± 6.5 1552.9 ± 7.1	51.7 ± 13.2 47.9 ± 4.3	14 12	Thomas (2025c) [11]
Zinnwald, Cassiterite	1313.9 ± 6.1 1332.7 ± 0.4	59.4 ± 19.1 4.3 ± 0.4	18 20	1521.5 ± 8.5 1581.5	70.0 ± 26.0 3.5	10 1	Thomas (2025a) [4]
Ehrenfriedersdorf, Beryl-vein	1328.6 ± 5.6 1322.8 ± 5.5	60.0 61.4 ± 18.9	14 10	1580.2 1571.8 ± 7.1	52.0 64.0 ± 14.4	10 10	Thomas et al. (2023b) [2]
E-Thuringia, Minette	1332.9 ± 10.2 1323.5 ± 2.4	71.6 ± 28.8 75.6 ± 10.9	10 15	1585.2 ± 6.2 1575.3 ± 5.8	68.0 ± 5.3 73.8 ± 9.9	10 15	Thomas and Recknagel (2024) [12]
Grey cast iron No. 2	1324.6 ± 11.8 1317.8 ± 10.0	66.9 ± 13.8 77.7 ± 15.8	12 12	1572.3 ± 9.5 1580.2 ± 7.1	42.0 ± 21.1 62.1 ± 22.7	12 12	Thomas et al. (2025a) [4]

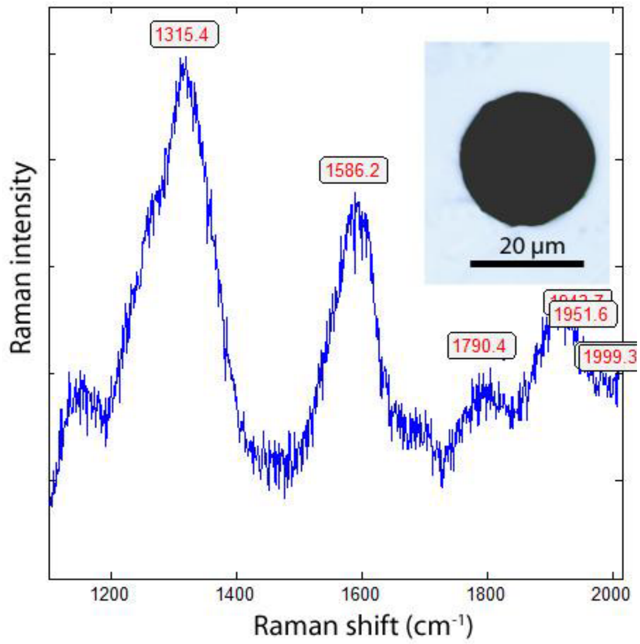

Figure 2a: Raman spectrum of lonsdaleite in fluorite in zinnwaldite from Zinnwald, taken at 30 mW on the sample [3].

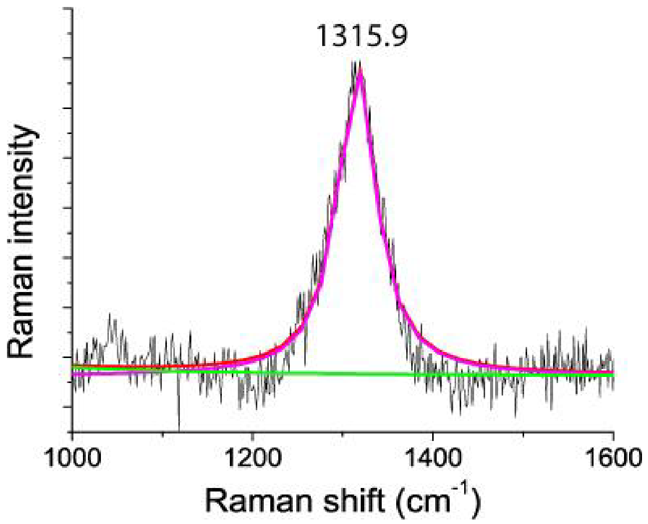

Figure 2b: Raman spectrum of a diamond-like compound taken at 4 mW on the fluorite sample from Zinnwald. The FWHM is 51.8 cm^{-1}. The "graphite band" is completely missing. Note that at about 30 mW on the sample, a strong graphite band at 1599 cm^{-1} becomes visible [3].

In Figure 2a, the Raman band of graphite at 1586 cm^{-1} is clear to see. Reducing the laser power to 4 mW on the sample allowed the graphite band to disappear totally (Figure 2b).

Initially, we have interpreted the black spherical and half-spherical crystals as lonsdaleite. The other lonsdaleite crystals from Sadisdorf/ Erzgebirge are more or less colorless and oblong [3]. The new Raman spectroscopic studies on the black crystals make it probable that they reflect a random substitution of B and N atoms in the diamond lattice [16] or contain amorphous diamond. Boron is present in the fluorite sample too [9]. Another reason for the black coloring is maybe the participation of more complex hydrocarbons like naphthalene [$C_{10}H_8$] [17] instead of methane in fluid inclusions. The cubic boron nitride (cBN) has its main band at 1304 cm^{-1}. Also, boron-doped diamond is a possibility [18]. Those new results (mixing of diamond with cBN) change nothing in the interpretation of the formation of this diamond-like compound in the upper crust. According to Zinin et al. (2009) [19], there are different mixtures in the B-C-N triangle possible. During new Raman measurements, we also found spherical boron crystals in the immediate vicinity of the diamond or diamond-like carbon (DLC) in fluorite from Zinnwald with an extreme band in the low-frequency range [20] at 73.8 cm^{-1} (similar to the natural diamond from Brazil with 76.6 cm^{-1}). Note, DLC is usually black and, in rare cases, colorless.

A more detailed description of the nature cases (without the new interpretations) is described in Thomas et al. (2025b) [9] and Thomas (2025a) [4] and references therein. Supercritical conditions for a substance (e.g., H_2, H_2O, CH_4, CO_2) occur when its temperature and pressure exceed its critical point, which leads to unique properties of fluids if they arrive at supercritical conditions (1000 to 2000°C – see Ni (2023) [21] and Ni et al., 2017) [22]. Above the critical point, substances possess the density of a liquid but the diffusivity and viscosity of a gas. This hybrid nature enables them to dissolve a broad range of compounds, and slight variations in pressure and temperature can often tune their solvation powers. That means that at temperatures over 550°C, the end of the magmatic and pegmatitic stage, all just called compounds are in the supercritical stage and are generally highly mixable, especially when the substances involved have similar molecular characteristics and are at the appropriate temperature and pressure conditions. However, not all combinations are fully miscible. That is an excellent possibility of a fractionated separation and extraction [14,23]. Supercritical fluids are superior to gases in their ability to dissolve materials like liquids or solids. Near the critical point, small changes in pressure or temperature result in significant changes in density, allowing many properties of a supercritical fluid to be "fine-tuned". Fine-tuning is the key to strong element fractionation during the crossing of the supercritical to the critical and undercritical stages. Samples of the "fine-tuning" we find in melt inclusions in granites, pegmatites, and high-temperature mineralizations (e.g., cassiterite mineralization). Some elements take extreme values at the solvus crest of a pseudobinary silicate-melt-water system and are then mainly Lorentzian distributed [24].

Discussion

We have shown in a couple of papers [25-27] that the processes of the formation of diamonds or diamond-like carbon (DLC) in cast iron, and also different minerals of the Earth's crust, have a certain similarity: formation apparent far away from the equilibrium conditions for diamond formation from graphite at about 5 GPa or more, and high temperatures. Supercritical fluids/melts may be the key medium for the formation of diamond and moissanite under non-equilibrium conditions. We call this process the supercritical-initiated CVD process, which may vary somewhat in nature or technique. That means the intentional growth of a defined diamond coating is disturbed by the very different targets. Through this process, the diamonds are also affected by the supercritical fluid (maybe also by hydrogen [28], which is responsible for the significant broadening of the first-order Raman band, indicated by a substantial increase in the FWHM (from about 4 to 50 cm^{-1} or more). That water-pure silicate melts do not influence the transport of diamond in zircon inclusions coming from the mantle region shows the small FWHM values for the diamonds found at the Saidenbach-reservoir (near Ehrenfriedersdorf/E-Erzgebirge), Rötzler (GFZ Potsdam, oral communication) – see Table 3. Also, the graphite band which is generally at about 1580 cm^{-1}, which is here completely absent (see Table 1).

In addition, we show ways for effective fractionation and enrichment of different ore-forming elements in the Earth's crust by the supercritical fluid state (e.g., Thomas et al. 2025b) [9]. For example, a lot of tin is transported with supercritical fluids as orthorhombic cassiterite.

Fazit: There are different ways to form diamonds: formation in the mantle depths (at high pressure and high temperatures), transport via supercritical fluids or supercritical melts into the Earth's crust, and formation at relatively low bulk pressure and high temperatures by reaction of supercritical CH_4- and H_2-bearing fluids with graphite during melting of cast iron or in nature by reaction of supercritical methane and H_2 with carbon. The possibility of the formation of diamond from metastable cementite (see Bhadeshia 2020) [29] should not be left out of sight. The formation of diamond and boron whiskers in high quartz from Zinnwald cannot be explained clearly. However, the primary presence of graphite is a prerequisite. Reaction of supercritical CH_4 moving along channels to primary graphite is a possible way. More sophisticated studies are necessary. It is important to emphasize that it is possible to differentiate between diamonds grown at equilibrium conditions at high pressure and high temperature and diamonds transported by SCFs or SCMs from mantle deeps to crustal levels or formed directly at the last region or formed at the productiosn of grey cast iron.

Table 3: Characteristics of diamond from the Saidenbach-reservoir/Erzgebirge.

Diamond in Zrn	First order (cm^{-1})	FWHM (cm^{-1})	n
	1330.51 ± 0.55	5.81 ± 1.23	41

Zrn – zircon; a graphite band is not present.

Acknowledgment

The author thanks Gregor Brümmer (Alzheim/Germany) and Adolf Rericha (Falkensee, Germany) for the intensive discussion on the problems of diamond genesis.

References

1. Thomas R, Davidson P, Rericha A, Recknagel U (2023a) Ultrahigh-pressure mineral inclusions in a crustal granite: Evidence for a novel transcrustal transport mechanism. *Geosciences* 13: 1-13.
2. Thomas R, Recknagel U, Rericha A (2023b) A moissanite-diamond-graphite paragenesis in a small beryl-quartz vein related to the Variscan tin-mineralization of the Ehrenfriedersdorf deposit, Germany. *Geoscience* 13: 1-13.
3. Thomas R, Trinkler M (2024) Monocrystalline lonsdaleite in REE-rich fluorite from Sadisdorf and Zinnwald/E-Erzgebirge, Germany. Geology, Earth and Marine Sciences 6: 1-5.
4. Thomas R (2025a) Diamond, diamond whisker, graphite, carbon, and coesite in a quartz crystal from Zinnwald, E-Erzgebirge. Geology, Earth and Marine Sciences 7: 1-6.
5. Brümmer G, Thomas R, Scheiblauer K, (2025a) The formation of tiny diamonds inside grey iron castings. Castings SA. 26(3): 30.
6. Zaitsev AM (2001) Optical Properties of Diamond. A Data Handbook. *Springer*. I-XI and 1-502 pages.
7. Prawer S, Nugent KW, Jamieson DN (1998) The Raman spectrum of amorphous diamond. *Diamond and Related Materials* 7: 106-110.
8. Bassett WA (2009) Diamond anvil cell, 50th birthday. *High Pressure Research* 29: 163-186.
9. Thomas R, Brümmer G, Scheiblauer K (2025b) Paradigm change of pegmatite formation -where does the water come from?. *Geology, Earth and Marine Sciences* 7: 1-7.
10. Thomas R (2024) ^{13}C-rich diamond in a pegmatite from Rønne, Bornholm Island: Proofs for the interaction between mantle and crust (2024). *Geology, Earth and Marine Sciences* 6: 1-3.
11. Thomas R (2025c) Diamond, diamond whisker, graphite, carbon, and coesite in a quartz crystal from Zinnwald, E-Erzgebirge. *Geology, Earth and Marine Sciences* 7: 1-6.
12. Thomas R, Recknagel U (2024) Lonsdaleite, diamond, and graphite in a lamprophyre: Minette from East-Thuringia/Germany. *Geology, Earth and Marine Sciences* 6: 1-4.
13. Thomas R, Webster JD (2000) Strong tin enrichment in a pegmatite-forming melt. *Mineralium Deposita* 35: 570-582.
14. Proctor JE (2021) The Liquid and Supercritical Fluid State of Matter. CRC Press. Taylor Francis Group. 276 pages.
15. Sengers J L (2002) How fluids unmix. Discoveries by the Shool of Van der Waals and Kamerlingh Onnes. Amsterdam. 302 pages.
16. Hubble HW, Kudryashov I, Solozhenko VL, Zinin PV, Sharma SK, et al. (2004) Raman studies of cubic BC_2N, a new superhard phase. *Journal of Raman Spectroscopy* 35: 822-825.
17. Hurai V, Huraiova M, Slobodnik M, Thomas R (2015) Geofluids – Developments in Microthermometry, Spectroscopy, Thermodynamics, and Stable Isotopes. Elsevier. Pg. 489.
18. Baker PA, Catledge SA, Harris SB, Ham KJ, Chen W, et al. (2018) Computational prediction and microwave plasma synthesis of superhard boron-carbon materials. *Materials* 11: 1-12.

19. Zinin PV, Liu XR, Ming LC, Sharma SK, Liu Y, et al. (2009) Ultraviolet and visible Raman spectroscopies of the graphitic BCx phases. *Diamond & Related Materials* 18: 1123-1128.

20. Beghi MG, Bottani CE (2004) Low-frequency Raman and Brillouin spectroscopy from graphite, diamond and diamond-like carbons, fullerenes and nanotubes. *Phil. Trans. R. Soc. Lond. A* 362: 2513-2535.

21. Ni H (2023) Introduction to advances in the study of supercritical geofluids. *Science China: Earth Science* 66(10): 2391-2394.

22. Ni H, Zhang L, Xiong X, Mao Z, Wang J (2017) Supercritical fluids at subduction zones: Evidence, formation conditions, and physicochemical properties. *Earth-Science Reviews* 167: 62-71.

23. Kortüm G, Buchholz-Meisenheimer (1952) Die Theorie der Destillation und Extraktion von Flüssikeiten. *Springer*. Pg: 381.

24. Thomas R, Rericha A (2024) Extreme element enrichment, according to the Lorentzian distribution at the transition of supercritical to critical and under-critical melt or fluids. *Geology, Earth and Marine Sciences* 6: 1-6.

25. Brümmer G, Thomas R, Scheiblauer K (2025b) Wie wächst er nun?. Der Graphit im Gußeisen unter dem Raman-Spektroskop. In press.

26. Thomas R, Brümmer G, Scheiblauer K (2025a) Unexpected carbon phases in grey cast iron – diamond, calcite, and methane. *Geology, Earth and Marine Sciences* 7: 1-6.

27. Thomas R (2025b) Boron in some Variscan deposits in the German Erzgebirge. *Geology, Earth and Marine Sciences*.

28. Rakha SA, Guojun Yu, Jianqing C (2012) Correlation between diamond grain size and hydrogen incorporation in nanocrystalline diamond films. *Journal of Experimental Naniscience* 7: 378-389.

29. Bhadeshia HKDH (2020) Cementite. *International Material Reviews* 65: 1-27.

Citation:

Thomas R (2025) Diamond in Pegmatites and Related Rocks in the Upper Crust. *Geol Earth Mar Sci* Volume 7(6): 1-5.